# Design of Neuro-Fuzzy based control of Synchronous generator

Raheel Aslam<sup>1</sup>, Alishah Khalid<sup>2</sup>, Abid Aman<sup>3</sup>, Toqeer Ahmed<sup>3</sup>, Kanwal Waqar<sup>3</sup>, Mohammad Rasel Amin<sup>3</sup>

<sup>1</sup>Department of Electrical Engineering, Pakistan Institute of Engineering and Applied
Sciences, Islamabad, Pakistan
ool of Ontoelectronic Engineering, Changchun University of Science and Technology, Zhongshan, Gu

School of Optoelectronic Engineering, Changchun University of Science and Technology, Zhongshan, Guangdong, China.
 School of Automation, South China University of Technology, Guangzhou, Guangdong, China.

Abstract- Improving the efficiency of synchronous generators is crucial for achieving significant energy savings in global electricity production, given that they contribute to approximately 95% of the world's power generation. This article explores the topic of controlling synchronous generators, providing a thorough theoretical foundation and simulation-based control strategies along with a complete framework. The synchronous generator model is first linearized and then state feedback control strategies are used. The research smoothly shifts to exploring neuro-fuzzy control, noting that linear models are not sufficient for describing the complexities observed in the

behavior of synchronous generators. The neuro-fuzzy controller was developed to address the system's non-linearities. Its improved performance is a result of its ability to simulate complex, non-linear systems better than conventional approaches. Nonlinearities are addressed by combining neuro-fuzzy intelligence with linear control. Stability and precision are improved by a control law that has been derived to counteract nonlinearities. The study highlights the neuro-fuzzy controller's adaptive characteristics in obtaining accurate output control under difficult nonlinear behavior in the generator system.

*Index Terms*- Neuro-Fuzzy, State feedback, Linear model, Nonlinear model, Lyapunov Stability

# I. INTRODUCTION

Synchronous generators are recognized for their longevity and dependability in providing steady power under many circumstances, making them essential in fulfilling the increasing demands for electricity worldwide [1]. Even with their importance, these generators are still difficult to fully optimize for grid stability and energy efficiency. Due to their nonlinear and dynamic character, they require complex control systems, which have historically relied on linearized models for stabilization. Nevertheless, standard methods are unable to fully capture the complex nonlinear behavior, which hinders achieving peak performance. Resolving this constraint is essential to guaranteeing the efficient operation and accurate control of electrical output in power generation

systems. A neuro-fuzzy is an advanced control system that improves the accuracy and flexibility of a system for controlling, by merging fuzzy logic and neural network techniques. The

system can efficiently manage uncertainties and nonlinearities thanks to this hybrid method, which also optimizes generator performance under a range of operating situations.in leading journals to complete their grades. In addition, the published research work also provides a big weight-age to get admissions in reputed varsity. Now, here we enlist the proven steps to publish the research paper in a journal.

In the literature, the comparison to Particle Swarm Optimization and conventional methods, including the use of a Biogeography-Based Optimization (BBO) algorithm to optimize PID parameters in a Power System Stabilizer (PSS) showed superior performance in minimizing low-frequency oscillations in a simulated single machine infinite bus system [2]. However, the BBO algorithm could have drawbacks like slow convergence and sensitivity in initial conditions. The neuro-fuzzy controller, on the other hand, uses its adaptive learning potential to improve performance and get past the problems with BBO. It turns out to be more accurate and efficient for controlling synchronous generators. In a related study, digital time simulations for a one-machine infinite bus test power system demonstrated that an Adaptive Neuro-Control System (ANCS) using neural networks for nonlinear generator control was more adaptable and effective in improving system damping than linear optimal and self-tuning regulators [3]. However there could be problems with overfitting and computational complexity with the ANCS. On the other hand, a neuro-fuzzy controller works better and more accurately for controlling synchronous generators. It does this by utilizing its enhanced adaptability to manage uncertainties and nonlinearity, which makes it a good substitute for ANCS in some situations.

The study smoothly combines a particular linearized model for synchronous generators with the neuro-fuzzy controller. The literature review emphasizes neuro-fuzzy control as a comprehensive strategy for controlling both linear and nonlinear components. Its superiority is confirmed by comparative analysis, providing a cost-effective way to optimize power generation control while resolving issues with traditional methods. [4].

The study develops a control law to reduce the nonlinearities of synchronous generators, enhancing accuracy and stability. An effective method for nonlinear dynamics

is obtained by combining this with state feedback control. The adaptive characteristics of the neuro-fuzzy controller are used to

show precise output control in difficult nonlinear circumstances. A complete solution for synchronous generator performance optimization is provided by this integrated method. [5].

Given the aforementioned steps, the following goals are stated for this research

paper:

- (1) To analyze and contrast state feedback control's efficiency for linearized synchronous generator models.
- (2) To create and put into use a neuro-fuzzy controller for the linearized model, allowing for precise output regulation and adaptive control.
- (3) To create a control law that efficiently reduces nonlinearities in the behavior of synchronous generators.
- (4) To integrate state feedback control with the nonlinear control law for improved stability.
- (5) To use the neuro-fuzzy controller on the controlled nonlinear model and determine whether it can sustain the necessary performance levels under nonlinear circumstances.

#### II. PROBLEM FORMULATION

The synchronous generator and issue statement is modeled both linearly and nonlinearly in this section.

# A. Dynamic Modeling

One of the most crucial aspects of modeling power systems is the modeling of synchronous generators. Several models are put forth in the literature [6] depending on the information that is available about the system. Due to its low computational expenses, decentralization is becoming more and more important in multimachine scenarios. Local implementation of the state estimate technique would be made possible by decentralization. System partitioning and the boundary of subsystems are essential to the decentralization process [7][8]. Furthermore, many decentralized synchronous machine models are employed, including the transient and sub-transient models [6][9]. The state equations listed below describe the characteristics of the transient synchronous machine model that is employed in this study.

$$\dot{\alpha} = \omega_{\rm B}(\omega - 1 - f_{\theta}) \tag{1}$$

$$\dot{\omega} = \frac{1}{M} [T_{\rm m} - T_{\rm e} - D_{\rm r}(\omega - 1) \tag{2}$$

where  $\omega_B$  is the starting value for  $\omega$ ,  $\omega$  is the per unit speed of the rotor, and  $f_\theta$  is the rate at which the angle of the terminal voltage phasor is changing.  $\alpha$  represents the angle of the generator's internal rotor with regard to the terminal voltage phasor, M is the mass inertia of the rotor,  $T_m$  is the mechanical torque produced by the turbine driving the generator,  $T_e$  is the electrical torque related to the power that the generator is required to supply and  $D_r$  is the coefficient for damping, to smooth our  $\omega$  oscillations in transient

conditions. These equations, often known as "swing equations" are crucial for stability. Conceptually,  $\omega$  and power system frequency are linked [10], and any changes to the power network have an impact on  $f_{\theta}$  and hence,  $T_{e}$ .

The following equations describe how the rotor of the generator works to generate voltage in the stator:

$$\dot{E}_{q} = \frac{1}{T_{do}} \left\{ E_{fd} - E_{q} - (X_{d} - X'_{d}) \left[ -\iota_{d} - \frac{k_{d2}}{X'_{d} - X_{ls}} \left( -(X'_{d} - X_{ls})\iota_{d} - E_{q} \right) \right] \right\} (3)$$

$$\dot{E}_{d} = \frac{1}{T_{qo}} \left\{ -E_{d} - \left( X_{q} - X'_{q} \right) \left[ -\iota_{q} - \frac{k_{q2}}{X'_{q} - X_{ls}} \left( \left( X'_{q} - X_{ls} \right) \iota_{q} - E_{d} \right) \right] \right\} (4)$$

$$E_{fd}^{\cdot} = \frac{1}{T_{\Lambda}} [k_{\Lambda}(\nu_{\text{ref}} - \nu_{\text{t}}) - E_{\text{fd}}]$$
 (5)

ISSN: 1673-064X

Whereas,

$$T_{\rm e} = k_{\rm a1} E_{\rm d} \iota_{\rm d} + k_{\rm d1} E_{\rm g} \iota_{\rm g} + (X_{\rm d}' - X_{\rm g}') \iota_{\rm d} \iota_{\rm q} \tag{6}$$

$$\begin{bmatrix} \iota_{\rm d} \\ \iota_{\rm q} \end{bmatrix} = z^{-1} \begin{bmatrix} r_s & -X'_{\rm q} \\ X'_{\rm d} & r_s \end{bmatrix} \begin{bmatrix} k_{\rm q1} E_{\rm d} - \overline{n} \nu_{\rm d} \\ K_{\rm d1} E_{\rm q} - \overline{n} \nu_{\rm q} \end{bmatrix}$$
(7)

$$z^{-1} = I^2 + \overline{n}^2 \begin{bmatrix} r_s & X_q' \\ -X_d' & r_s \end{bmatrix}^{-1} \begin{bmatrix} r_T & X_T \\ -X_T & r_T \end{bmatrix}$$
(8)

$$\begin{bmatrix} v_{\text{td}} \\ v_{\text{tq}} \end{bmatrix} = \overline{n}^2 \begin{bmatrix} r_T & X_T \\ -X_T & r_T \end{bmatrix} \begin{bmatrix} t_d \\ t_q \end{bmatrix} + \overline{n} \begin{bmatrix} v_d \\ v_q \end{bmatrix}$$
(9)

The direct axis and quadrature axis voltages are calculated as

$$v_{t} = \sqrt{v_{td}^{2} + v_{tq}^{2}}, \quad v_{d} = -v\sin\alpha, \quad v_{q} = v\cos\alpha$$

$$v = -(v_{v} - v_{y}), \quad f_{\theta} = -(f_{v} - f_{y}), \quad \alpha = \delta - \theta$$

It is evident that this state variable uses the internal rotor angle  $(\alpha)$  rather than the rotor angle  $(\delta)$ . This choice was based on the fact that, in a model of a multimachine power system, each generator's rotor angle  $(\delta_i)$  and stator voltage phase  $(\theta_i)$ , which are crucial for the generator's internal parameters, are determined with reference to a common reference frame. Nevertheless, it would be counterproductive in a decentralized setting to know the values of these figures without also being aware of the common reference frame [11]. To deal with this, the internal rotor angle might be utilized as a state variable.

# B. Output Equations

The measurement outputs at the HV bus are the active power output  $(P_y)$ , the reactive power output  $(Q_y)$ , the current magnitude  $(\iota_y)$ , and its phase with respect to the voltage phasor  $(\theta_{\iota y})$ . The stator current measured phase  $(\theta_{\iota y})$  and its measured magnitude  $(\iota_y)$  with respect to the voltage phasor are the measurements that are regarded as system outputs. The following equations yield these:

$$\iota_{y} = \overline{n} \sqrt{\iota_{q}^{2} + \iota_{d}^{2}} \tag{10}$$

$$\theta_{\iota y} = \alpha + \tan^{-1} \left( \frac{\iota_d}{\iota_q} \right) \tag{11}$$

and  $(\iota_d)$ ,  $(\iota_q)$  are given by (7) and due to its close relationship to speed, frequency measurement  $(f_{sys})$  has also been taken into account; it's per unit value is:

$$f_{\rm sys} = \omega$$
 (12)

Attempting to increase the accuracy of the unknown input estimation can be facilitated by further measurements [12]. Regarding the measurable quantities, the decentralized model used here permits the use of extra quantities as measurements (unlike, say, the model in [12]), however this depends on the model that is applied. Since this can be done using the decentralized model employed here, the prior case studies have

been reexamined, taking into account the additional measurements that can be made by Phase Measuring Units (PMUs) (active and reactive power) [12]. The following are

the measurement functions for these:

$$[P_y = E_d \iota_d + E_q \iota_q + (X_d' - X_q') \iota_d \iota_q - (\iota_d^2 + \iota_q^2) (Rs + \overline{n}RT)$$
(13)

$$[Q_y = E_d \iota_q - (X_q' + \overline{n}^2 X_T) \iota_q^2 - (X_d' + \overline{n}^2 X_T) \iota_d^2 - E_q \iota_d$$
 (14)

where  $P_y$  and  $Q_y$  represent the generator's terminal bus-measured active and reactive power, respectively. The ratios of constants given in above equations are given as following:

$$k_{d1} = \frac{(X_d'' - X_{ls})}{(X_d' - X_{ls})} \tag{15}$$

$$k_{d2} = \frac{(X_d' - X_d'')}{(X_d' - X_{ls})} \tag{16}$$

$$k_{q1} = \frac{\left(X_{q}^{"} - X_{ls}\right)}{\left(X_{q}^{'} - X_{ls}\right)} \tag{17}$$

$$k_{q2} = \frac{(X_q' - X_q')}{(X_q' - X_{Is})} \tag{18}$$

By taking into account  $X_q'' = X_q'$  and  $X_d'' = X_d'$ , it is possible to construct the transient model since  $k_A = 1$ ,  $k_{q1} = k_{d1} = 1$  and  $k_{q2} = k_{d2} = 0$  in this situation the Eqns. (3),(4),(5),(6),(7) becomes

$$\dot{E}_{q} = \frac{1}{T_{do}} \left\{ E_{fd} - E_{q} - (X_{d} - X_{d}')[-\iota_{d}] \right\}$$
 (19)

$$\dot{E}_{d} = \frac{1}{T_{qo}} \left\{ -E_{d} - (X_{q} - X'_{q}) [-\iota_{q}] \right\}$$
 (20)

$$E_{fd}^{\cdot} = \frac{1}{T_{\Delta}} [(\nu_{ref} - \nu_{t}) - E_{fd}]$$
 (21)

$$T_{\rm e} = E_{\rm d}\iota_{\rm d} + E_{\rm q}\iota_{\rm q} + \left(X_{\rm d}' - X_{\rm q}'\right)\iota_{\rm d}\iota_{\rm q} \tag{22}$$

$$\begin{bmatrix} \iota_{\rm d} \\ \iota_{\rm q} \end{bmatrix} = Z^{-1} \begin{bmatrix} r_s & -X_{\rm q}' \\ X_{\rm d}' & r_s \end{bmatrix} \begin{bmatrix} E_{\rm d} - \overline{n} \nu_{\rm d} \\ E_{\rm q} - \overline{n} \nu_{\rm q} \end{bmatrix}$$
(23)

C. State Space Representation

The following are the state, input, and output vectors:

$$x = [x_1 \quad x_2 \quad x_3 \quad x_4 \quad x_5]^{T} = [\alpha \quad \omega \quad E_q \quad E_d \quad E_{fd}]^{T}$$

$$u = [u_1 \quad u_2 \quad u_3 \quad u_4]^{T} = [T_m \quad v_{ref} \quad v \quad f_{\theta}]^{T}$$

$$y = [y_1 \quad y_2 \quad y_3 \quad y_4 \quad y_5]^{T} = [f_{sys} \quad \iota_y \quad \theta_{\iota y} \quad P_y \quad Q_y]^{T}$$

Using the aforementioned variables to build the state space model, the following model is derived

$$\dot{x} = \overline{A}x + \overline{B}u + \theta(x, u) \tag{24}$$

$$y = \overline{C}x + \overline{D}u \tag{25}$$

where the disturbance vector,  $d \in \mathbb{R}^{kd}$ , is present. The matrices  $\overline{A}, \overline{B}, \overline{C}$  and  $\overline{D}$  can be represented as uncertain matrices with compatible dimensions.

$$\overline{A} = \overline{A}_{o} + A_{o}, \qquad \overline{B} = \overline{B}_{o} + B_{o},$$

$$\overline{C} = \overline{C}_{o} + C_{o}, \qquad \overline{D} = \overline{D}_{o} + D_{o},$$

Consequently, after being rearranged in terms of the state and the input vector, The linear terms of the state equations yield the  $A_o$  and  $B_o$  matrices, which are given as follows:

the output equations around the nominal operating point have been linearized, *Co* and *Do* are obtained. Given below are the function  $\theta(x, u) = [\theta 1(x, u)\theta 2(x, u)\theta 3(x, u)\theta 4(x, u)\theta 5(x, u)]^T$ 

Whereas.

$$\theta 1(x, u) = 0, \theta 2(x, u) = \frac{-T_e}{M}, \theta 3(x, u) = \frac{1}{T_{do}} (X_{d^l d} + X'_{d^l d})$$
$$\theta 4(x, u) = \frac{1}{T_{do}} (-X_q \iota_q + X'_q \iota_q), \theta 5(x, u) = \frac{1}{T_A} (k_A (-\nu_t))$$

The estimated values of the constants in matrices  $A_o$ ,  $B_o$  and using the nominal operating point by calculating the values of the matrices  $C_o$  and  $D_o$  using the Jacobian block in the MATLAB.

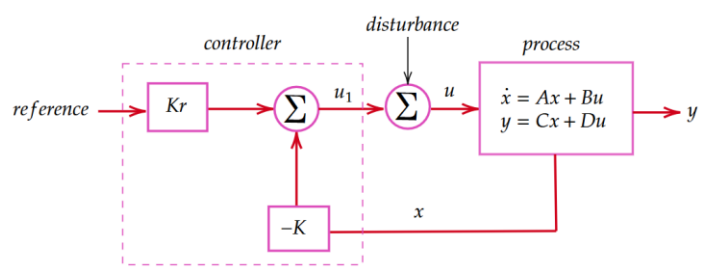


Figure 1 State feedback Control System.

## D. State Feedback Controller

Controlling dynamic systems requires the use of a state feedback controller, a fundamental concept in control theory and engineering. It is an approach for controlling systems that entails using direct feedback from the system's internal state variables to alter behavior to achieve desired performance [13].

Fig. 1 demonstrates a conventional control system state feedback diagram. The reference input, r, the controller components, K and  $k_r$ , the process disturbances, d, and the process dynamics, which are believed to be linear, make up the complete system. The feedback controller's goal is to regulate the system's output y, so

that, in situations of disturbances and uncertainty in the process dynamics, it follows the reference input.

The feedback can be expressed as follows if it is restricted to be linear

$$u_1 = k_r r - k x \tag{26}$$

Following the application of the feedback (26) to the linear system of (24), the closed loop system is produced as follows

$$\dot{x} = (A_o - B_o k)x + B_o kr \tag{27}$$

Let  $\mu_1, \mu_2, ..., \mu_n$  be the desired eigenvalues. K must be computed such away that the closed loop eigenvalues should be  $\mu_1, \mu_2, ..., \mu_n$  For the closed-loop system, in particular, the equilibrium point and steady-state output are given by

$$xe = (A_o - B_o k)^{-1} B_o kr (28)$$

$$ye = C_0 x_e \tag{29}$$

Thus,  $k_r$  ought to be selected so that ye = r (the intended output value) is achieved.  $K_r$  is a scalar, thus it can easily be solved to demonstrate

$$kr = -\frac{1}{C_o(A_o - B_o k)^{-1} B_o}$$
 (30)

Keep in mind that  $k_r$  is the exact opposite of the closed loop system's zero frequency gain. Therefore, the dynamics are tailored for the closed-loop system to achieve the objective by using the gains K and  $k_r$ .

In the context of this study, the Lyapunov Function Candidate (LFC), designated as V(x), which is a key notion in the analysis of dynamic systems. An LFC has the following characteristics:

- (1) Continuity: V(x) should be real-valued continuous function.
- (2) Positive Definiteness: V(x) > 0, it should be a positive definite function.
- (3) Negative Definiteness: V(x) < 0, it should be a negative definite function.

In this study, the simple linear model is as follows:

$$\dot{x} = A_o x + B_o u \tag{31}$$

$$y = C_0 x \tag{32}$$

It can confidently be simplified by the control law for the purposes of the stability proof because the pre-gain factor  $k_r$  has little effect on system stability, leading to the reduced formulation shown below.

$$u_1 = -Kx \tag{33}$$

Substituting the values from equation 33 into equation 31 the following expression for further analysis is obtained.

$$\dot{x} = A_o x + B_o(-Kx) \tag{34}$$

$$\dot{x} = (A_o - B_o K) x \tag{35}$$

For analysis purposes, the Lyapunov function is defined as follows:

$$V = \frac{1}{2}x^T x \tag{36}$$

Indeed, V(x) is assumed to be a positive definite function in the analysis, satisfying V(x) > 0.

$$\dot{V} = \frac{1}{2} \left( \dot{x^T} x + x^T \dot{x} \right) \tag{37}$$

$$\dot{V} = \frac{1}{2} \left( 2\dot{x}^T x \right) \tag{38}$$

$$\dot{V} = \left( \dot{x}^T x \right) \tag{39}$$

$$\dot{V} = (x^T x) \tag{39}$$

Substituting the values from Equation 35 into Equation 39, the results are expressed as follows:

$$\dot{V} = \left( (A_o - B_o K) x \right)^T x) \tag{40}$$

$$\dot{V} = x^{T} (A_{o}^{T} - K^{T} B_{o}^{T}) x \tag{41}$$

If the matrix K is chosen such that the eigenvalues of (A -BK) < 0, then it can be asserted that  $\dot{V} \leq 0$ .

## E. Control Law for Non-Linear model

The control law developed in this study exhibits a surprising quality in that it successfully reduces the effects of the system dynamics' intrinsic nonlinearity [14]. The resulting control method produces a system response that closely resembles linearity by deftly canceling out the nonlinear terms as explained in equation 24. This distinctive feature offers a substantial addition to the field of nonlinear control and lays the groundwork for further research and application in complex systems. It also holds tremendous potential for improving system stability and performance. The following control law has been derived:

$$u_1 = k_r r - k x - (B_0^T B_0)^{-1} B_0^T \sigma \theta(x, u)$$
 (42)

Whereas.

$$\sigma = B_o(B_o^T B_o)^{-1} B_o^T)^{-1} (43)$$

The identity matrix is represented by the equation:

$$B_o(B_o^T B_o)^{-1} B_o^T \sigma = I(44)$$

Equations 42 and 43 can be substituted for equation 24, which causes a transformation that effectively cancels out the nonlinearity terms and yields a shortened expression that represents the intended linear behavior. This tactical substitution is crucial to this study since it helps to go around the system dynamics' complexity and concentrate on the more manageable linear features for further research and control scheme development. Nonlinearities can be generically divided into continuous and discontinuous categories. They can also be categorized as known or unknown [15].

**Assumption 1**: It is assumed that the non-linearity  $\theta(x, u)$  in the system is Continuous.

Substituting (42) and (43) into (24) simplifies it and eliminates nonlinearity, yielding:

$$\dot{x} = A_o x + B \left( k_r r - k x - (B^T B)^{-1} \sigma \theta(x, u) \right) + \theta(x, u) \tag{45}$$

$$\dot{x} = (A_o - B_o k) x + B_o k_r - B_o (B_o^T B_o)^{-1} B_o^T \sigma \theta(x, u) + \theta(x, u)$$
(46)

The equation has the following form once nonlinearity components are eliminated:

$$\dot{x} = (A_o - B_o k)x + B_o k_r \tag{47}$$

This form represents a linear term in the analysis and is equivalent

The development of phase portraits based on various initial conditions allows one to illustrate the stability of the system. These visual depictions give users a concrete way to evaluate the system's performance across various initial states. The empirical evidence is shown to support the stability of the system by analyzing trajectory patterns and convergence, which also supports the correctness of the theoretical approach [16]. Phase portraits, in this research, essentially act as a crucial link between theory and empirical validation. Fig. 2-5 depicts the phase portrait of all possible state combinations in this study in vivid detail. Notably, the convergence of all states towards the equilibrium points at zero is demonstrated by this thorough visual phase portrait, which provides persuasive proof. The stability of the designed control law is unmistakably highlighted by this collective behavior, providing strong empirical support for its effectiveness in maintaining system stability. The conceptual foundations of this research are strengthened by this empirical validation, which increases confidence in the efficiency of the suggested control technique to preserve system stability.

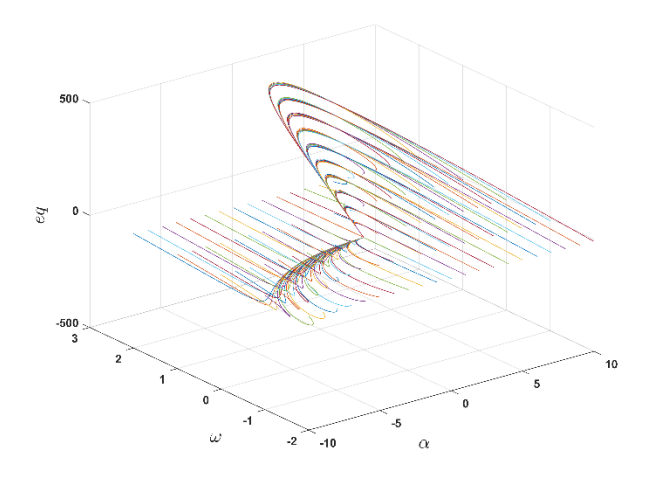


Figure 2 Phase portrait between  $\alpha$ ,  $\omega$ , eq.

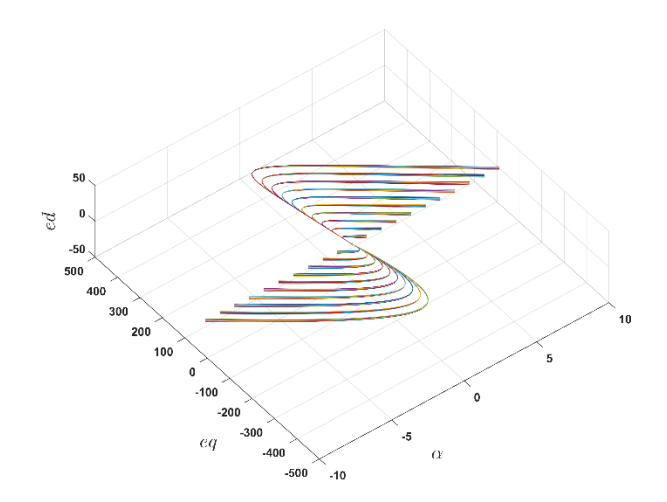


Figure 3 Phase portrait between α, eq, ed.

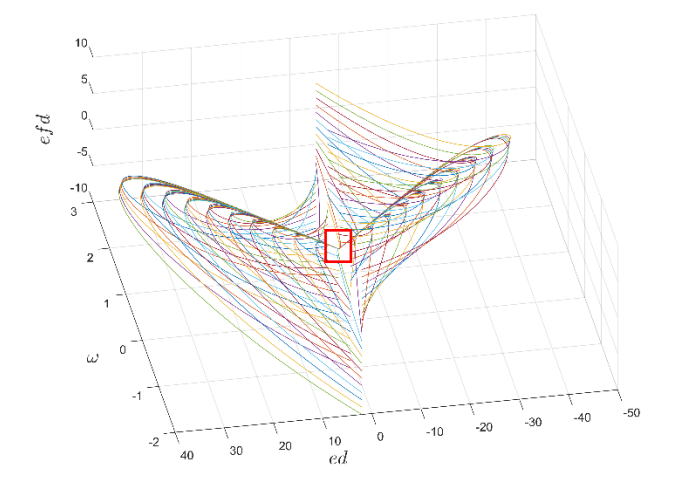


Figure 4 Phase portrait between  $\omega$ , ed,  $e_{fd}$ .

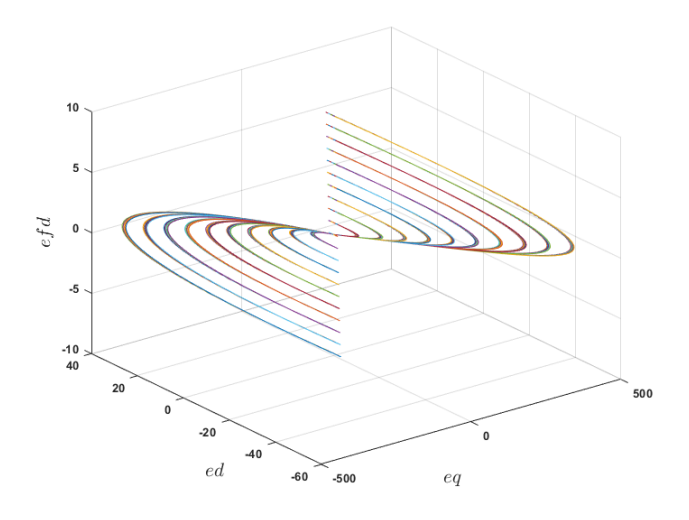


Figure 5 Phase portrait between eq, ed,  $e_{fd}$ .

## E. Neuro Fuzzy Controller

An effective computing system that combines fuzzy logic and neural networks, the neuro-fuzzy controller, exhibits improved flexibility and decision making. In particular, a hybrid learning technique is used by the adaptive neuro-fuzzy inference systems (ANFIS), which are motivated by the work of Sugeno and Tsukamoto [17]. The combination of neural network adaptability and fuzzy logic makes ANFIS a powerful instrument for smart and trustworthy control solutions in modern research. ANFIS is particularly good at handling uncertainty-related problems; it uses its flexibility to handle complicated situations with imprecise or unclear data. Despite their strength, neural networks have trouble processing imprecise data and are not very interpretable. These drawbacks are addressed by the incorporation of neural networks into neuro-fuzzy systems, like ANFIS, which improves flexibility and decision. This hybrid strategy is essential for developing intelligent and understandable control solutions, especially in situations involving complicated problems and ambiguous data.

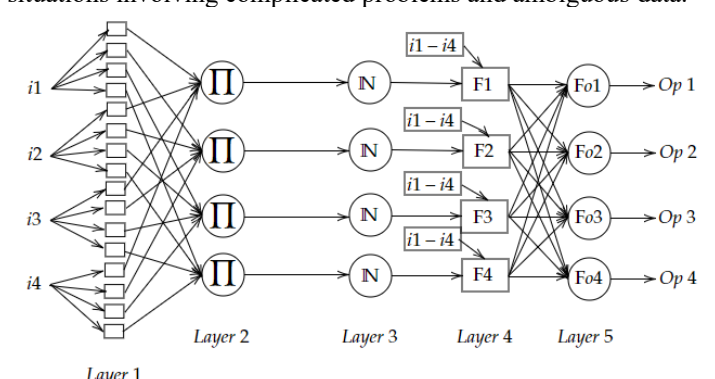


Figure 6 Basic Multilayer Multioutput Neuro-Fuzzy Model.

The fundamental model of the neuro-fuzzy inference system is shown in Fig. 6. The fuzzy inference system makes use of the first-order Sugeno fuzzy model, which has four inputs  $(i_1, i_2, i_3, \text{ and } i_4)$  and four related outputs  $(o_1, o_2, o_3, \text{ and } o_4)$ . This model is governed by the following set of rules:

**Rule1:** If  $i_1$  is  $A_1$ ,  $i_2$  is  $B_1$ ,  $i_3$  is  $C_1$ , and  $i_4$  is  $D_1$ , then the output  $o_1$  is determined by the equation:

$$f_1 = p_1 i_1 + q_1 i_2 + r_1 i_3 + s_1 i_4 + t_1$$

**Rule2:** If  $i_1$  is  $A_2$ ,  $i_2$  is  $B_2$ ,  $i_3$  is  $C_2$ , and  $i_4$  is  $D_2$ , then the output  $o_2$  is calculated as:

$$f_2 = p_2 i_1 + q_2 i_2 + r_2 i_3 + s_2 i_4 + t_2$$

**Rule3:** If  $i_1$  is  $A_3$ ,  $i_2$  is  $B_3$ ,  $i_3$  is  $C_3$ , and  $i_4$  is  $D_3$ , then the output  $o_3$  is determined using the equation:

$$f_3 = p_3 i_1 + q_3 i_2 + r_3 i_3 + s_3 i_4 + t_3$$

**Rule4:** If  $i_1$  is  $A_4$ ,  $i_2$  is  $B_4$ ,  $i_3$  is  $C_4$ , and  $i_4$  is  $D_4$ , then the output  $o_4$  is derived from the equation:

$$f_4 = p_4 i_1 + q_4 i_2 + r_4 i_3 + s_4 i_4 + t_4$$

The estimated weights and parameters for various datasets are represented in (48), which summarizes the outputs of the neuro-fuzzy inference system. It shows how flexible the system is to changing data, indicating its capacity to modify internal settings for optimum performance across various outputs.

## 1) laver 1

Each input node in this layer serves as an adaptive component that creates a membership grade corresponding to a linguistic label. This layer has a fuzzy quality, with  $i_1$ ,  $i_2$ ,  $i_3$ , and  $i_4$  acting as the system's inputs and  $O_{l,m}$  designating the mth node's output in layer 1. It should be noted that every adaptive node appears as a square node with a square function as shown in Eq. 48-51:

$$O_{1,m} = \mu_{i_1,m}$$
 for  $m = 1,2,3,4$  (48)

$$O_{1,n} = \mu_{i_2,n}$$
 for  $n = 1,2,3,4$  (49)

$$O_{1,o} = \mu_{i_3,m}$$
 for  $o = 1,2,3,4$  (50)

$$O_{1,p} = \mu_{i_4,m}$$
 for  $p = 1,2,3,4$  (51)

$$\mu_{i_1 m}(i_1) = \max \left[ \min \left( \frac{i_1 - w_m}{x_m - w_m}, \frac{y_m - i_1}{y_m - x_m} \right), 0 \right]$$
 (52)

where  $(w_m, x_m, y_m)$  are the parameters of the gaussian bell shaped membership function represented by eq 53.

$$\mu_{i_1 m}(i_1) = \frac{1}{1 + \left(\frac{i_1 - y_m}{w_m}\right)^2 x_m}$$
 (53)

## 2) layer 2

This layer is used to evaluate the weights connected to each membership function. It uses input values from the first layer, designated as  $i_{1m}$ , and performs membership calculations to represent the fuzzy sets corresponding to the relevant input variables.

$$O_{2,m} = w_m = \mu_{i_1,m}(i_1) \cdot \mu_{i_2,n}(i_2) \cdot \mu_{i_3,o}(i_3) \cdot \mu_{i_4,p}(i_4)$$
for  $m, n, o, p = 1,2,3,4$  (54)

## *3) layer 3*

Each node in this layer, denoted by a circle with the letters N, stands for the normalization of the firing intensity from the layer before. To determine the amount of activation for each fuzzy rule, this layer performs pre-condition matching. This layer's node count is equal to the number of fuzzy rules. Every node figures out the strength of the  $i^{th}$  rule in relation to the total strength of all firing rules.

$$O_{3,m} = \overline{w}_m = \frac{w_1}{w_1 + w_2 + w_3 + w_4}$$
 for  $m = 1,2,3,4$  (55)

For reliability, the outputs of this layer will be referred to as normalized firing strengths.

This layer provides the output values  $O_{4,m}$ , which are inferred using fuzzy rules. The output is a simple product of the first-order polynomial and the normalized firing rule strength. The node function is used to express the weighted output of a rule as follows:

$$O_{4,m} = \overline{w}_m f_m = \overline{w}_m (p_m i_1 + q_m i_2 + r_m i_3 + s_m i_4 + t_m)$$
 (56)

This layer, also known as the "output layer" collects all of the inputs from layer 4 and transforms the results of fuzzy categorization into precise, distinct values. Eq. 48 instructs the node on this layer to compute the total of all incoming signals.

$$\sum_{i=1}^{4} O_{5,m} = \frac{w_{i1} f_{i1} + w_{i2} f_{i2} + w_{i3} f_{i3} + w_{i4} f_{i4}}{w_{i1} + w_{i2} + w_{i3} + w_{i4}}$$
 (55)

For the aim of estimating the membership function, the neuro-fuzzy controller uses a hybrid learning method that combines the concepts of least squares estimate and backpropagation. This original strategy, described in this research, demonstrates the adaptability and flexibility of controller in obtaining precise and reliable fuzzy model parameterization. The integrated visualization is shown for the neuro-fuzzy controller in Fig. 7 that

has been rigorously trained using dataset data from the output results of state feedback controllers used in both linear and nonlinear systems. With the help of empirical data collected across a range of system dynamics, this figure highlights the crucial role the neuro-fuzzy controller plays in the system. It also highlights its adaptability and optimization potential.

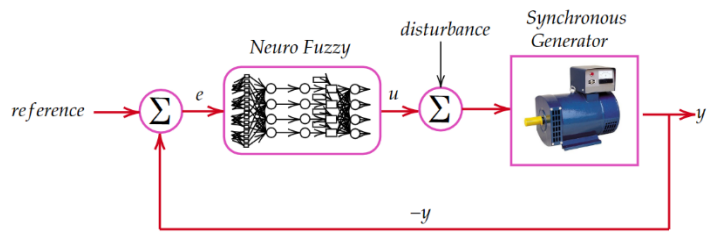


Figure 7 Neuro Fuzzy as a controller.

#### III. RESULTS

The outcomes of applying state feedback control with a carefully selected K matrix based on intended pole placement are shown in Fig. 8. The most important conclusion to draw from these findings is that all system outputs successfully converge in the direction of the desired reference step input. This shows that the state feedback controller for linear system functions effectively.

This effective tracking of the required reference signal highlights the utility of control strategy in real-world applications. It's a noteworthy accomplishment that emphasizes the applicability of the approach that is used to govern dynamic systems.

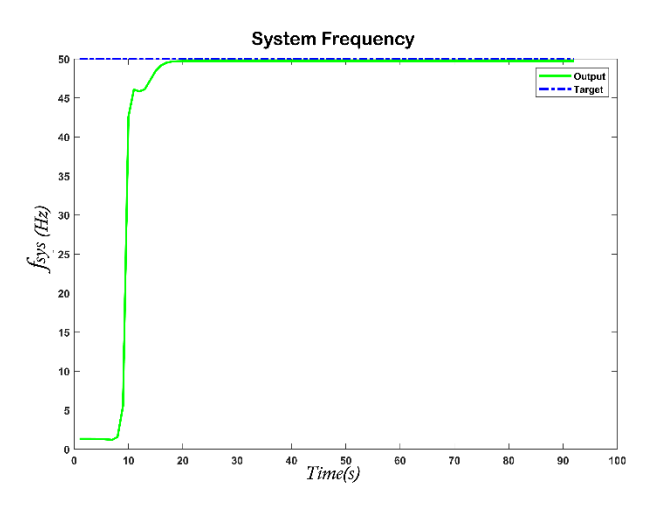


Figure 9 Neural Network result for  $f_{sys}$ .

The output responses of a neural network trained using the dataset produced by the state feedback controller are shown in Fig. 9 -13. The findings show that there is a need for improvement, even though the outputs show some degree of tracking to the specified reference input. Notably, it is seen that the error term and tracking response converge to the target values quite slowly. As a result, it was decided that changes were required to improve the system's functionality. The addition of a neuro-fuzzy controller then led to an improvement in tracking accuracy. This effective tracking of the required reference signal highlights the utility of control strategy in real-world applications. It's a noteworthy accomplishment that emphasizes the applicability of the approach that is used to govern dynamic systems.

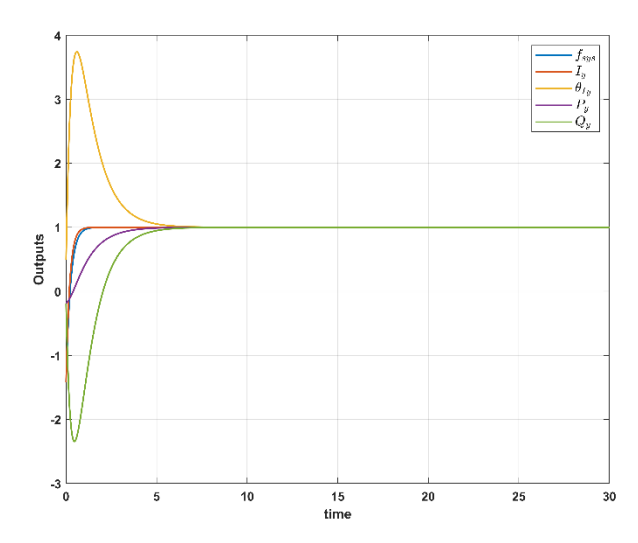


Figure 8 State feedback Linear model results for  $f_{sys}$ ,  $I_v$ ,  $\theta_{Iv}$ ,  $P_v$  and  $Q_v$ .

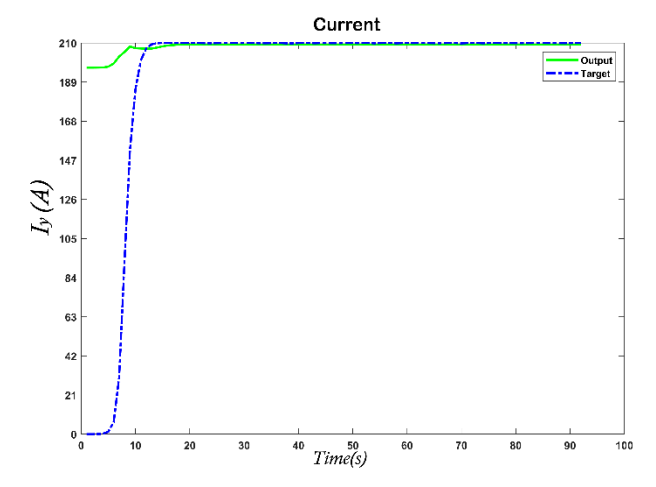


Figure 10 Neural Network result for I<sub>v</sub>.

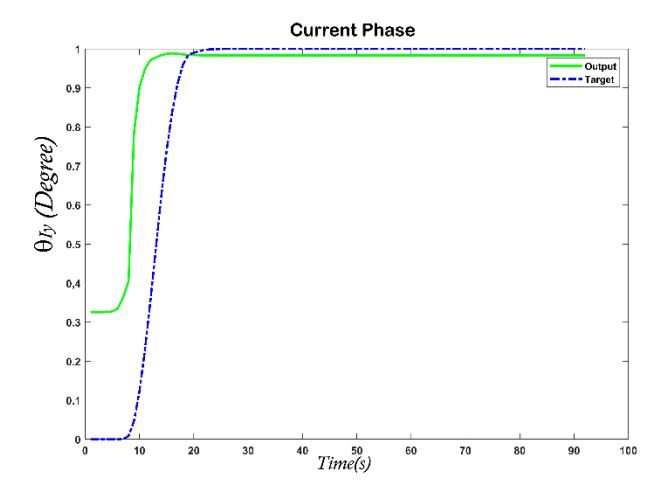


Figure 11 Neural Network result for  $\theta_{Iv}$ .

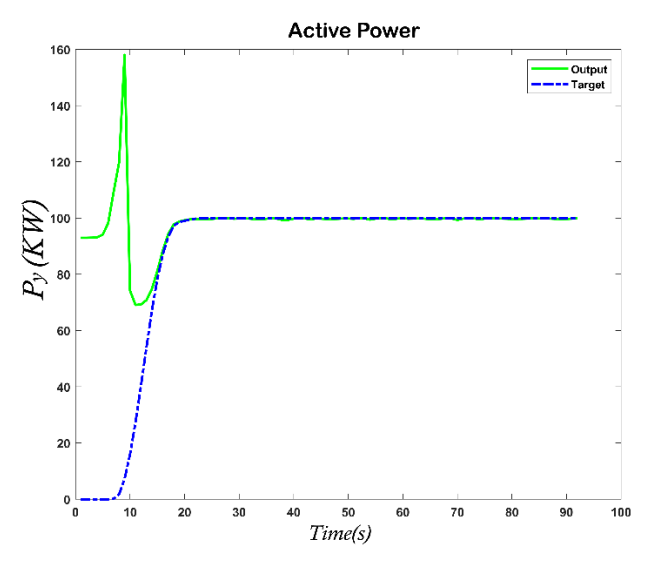


Figure 12 Neural Network result for  $P_{y}$ .

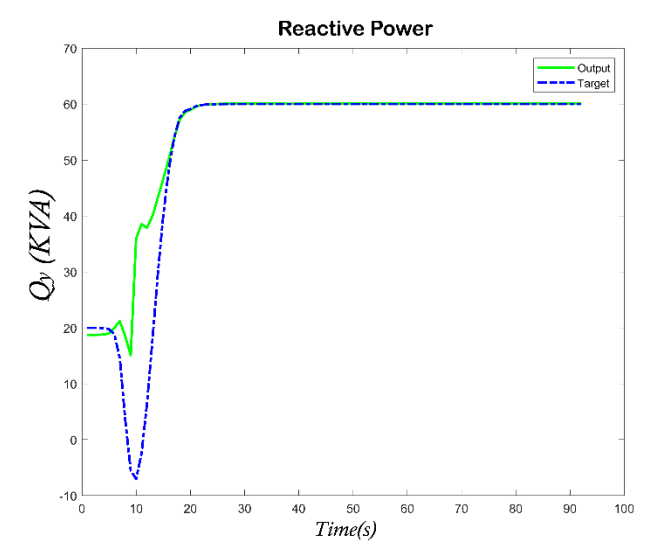


Figure 13 Neural Network result for  $Q_{\gamma}$ .

The output responses of the linearly trained neuro-fuzzy controller are shown collectively in Fig. 14 - 18. These outcomes clearly show a noteworthy accomplishment in this research, where a significant portion of the required output references have been successfully attained.

This finding reinforces the effectiveness of the control methodology and confirms its capability of achieving the desired performance goals. It demonstrates the effective use of the neuro-fuzzy controller in controlling the system and provides important insights into the flexibility and precision of the approach.

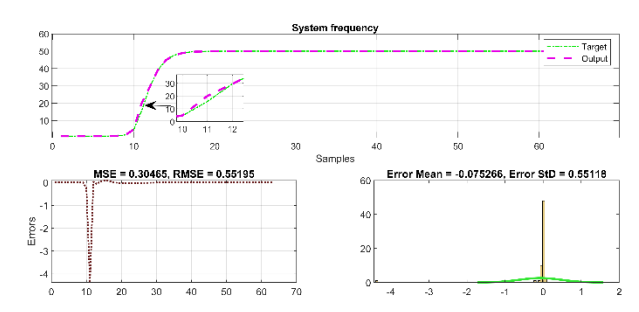


Figure 14 Neuro Fuzzy controller Output for  $f_{sys}$  Output.

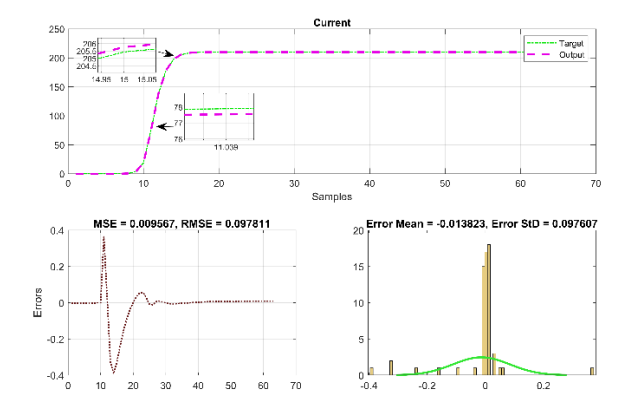


Figure 15 Neuro Fuzzy controller Output for I<sub>v</sub> Output.

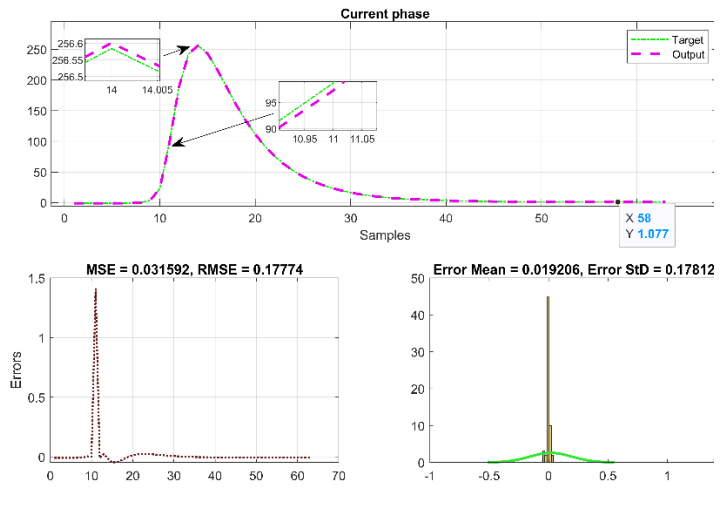


Figure 16 Neuro Fuzzy controller Output for  $\theta_{IV}$  Output.

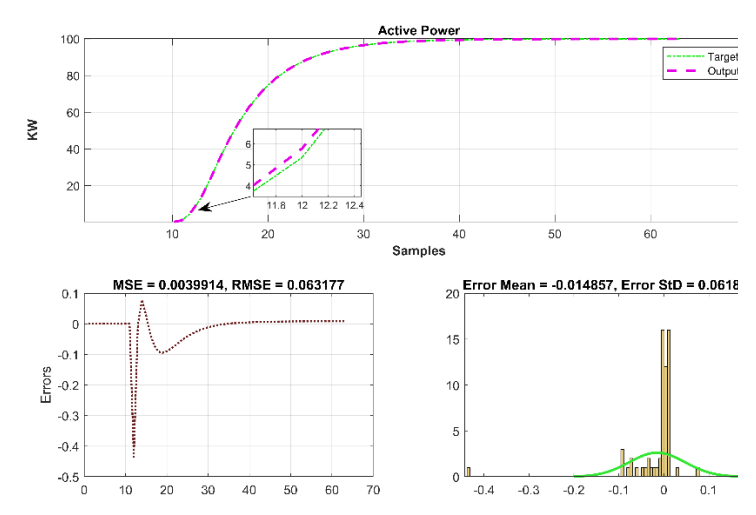


Figure 17 Neuro Fuzzy controller Output for P<sub>v</sub> Output.

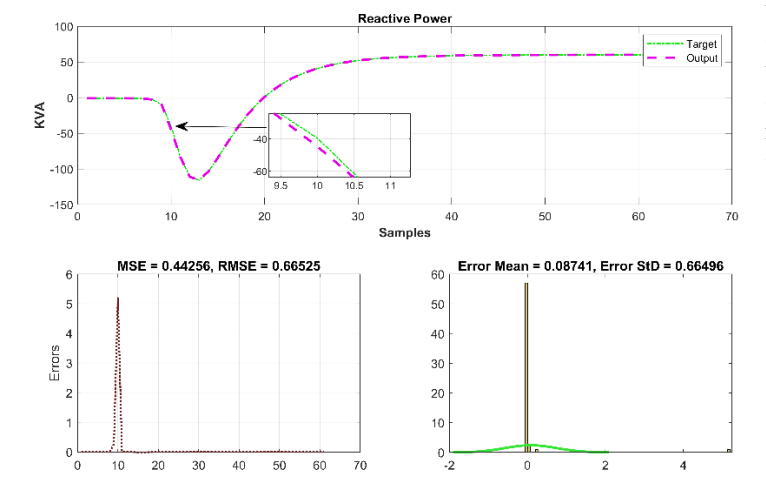


Figure 18 Neuro Fuzzy controller Output for Q<sub>v</sub> Output.

Fig. 19 depicts the outcomes of applying the control law to the nonlinear system and how well they coincide with the reference step input. It is crucial to remember that certain errors continue as a result of transients and residual nonlinearities in the system. However, these little differences are regarded as acceptable in the context of this study. They highlight the practical difficulties in regulating nonlinear systems while also supporting the effectiveness of control strategy in significantly reducing these difficulties.

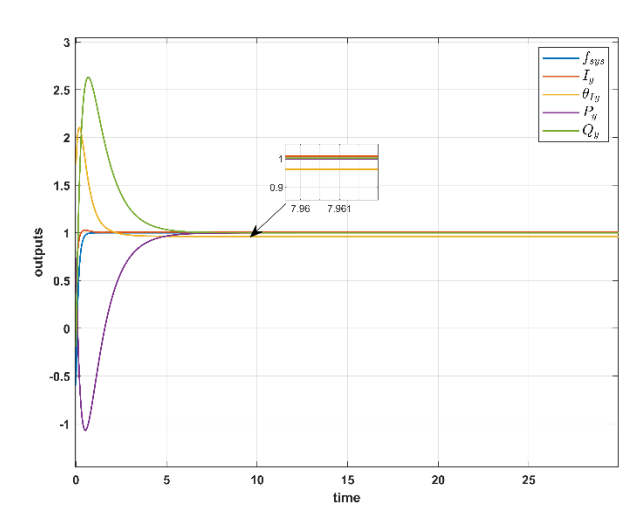


Figure 19 Controlled Non-Linear model result for  $f_{sys}$ ,  $I_y$ ,  $\theta_{Iy}$ ,  $P_y$  and  $Q_y$ .

The output responses produced by the neuro-fuzzy controller in this nonlinear system are completely depicted in the Fig. 20 to 24 that follow. Notably, compared to those of the linear system, the mean square error (MSE) values in these nonlinear tests are seen to be higher. The existence of transients inside the nonlinear system and the persistence of residual nonlinearities are to blame for this mismatch in MSE. These findings illustrate the complexity of nonlinear systems and the difficulties they present to control theories. The neuro-fuzzy controller shows its adaptability and effectiveness in controlling the nonlinear dynamics, underscoring the potential of this approach in the context of nonlinear system control. The performance may show some deviations from the reference signals as a result of these complexities, but it is important to emphasize that this is only temporary.

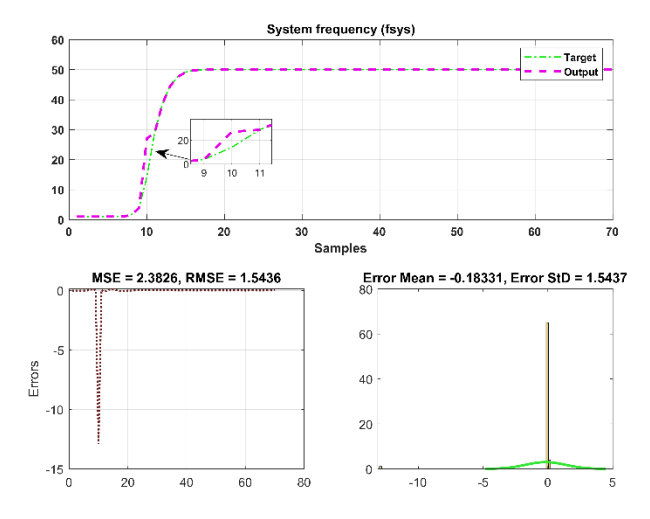


Figure 20 Neuro Fuzzy non-linear model control output for  $f_{sys}$ .

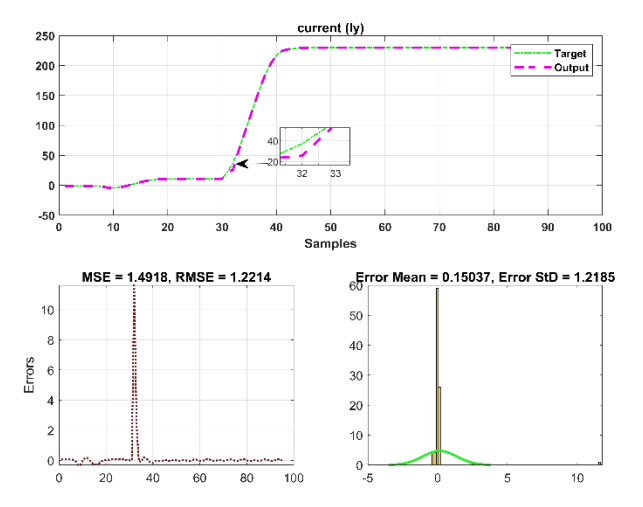


Figure 21 Neuro Fuzzy non-linear model control output for  $I_{\nu}$ .

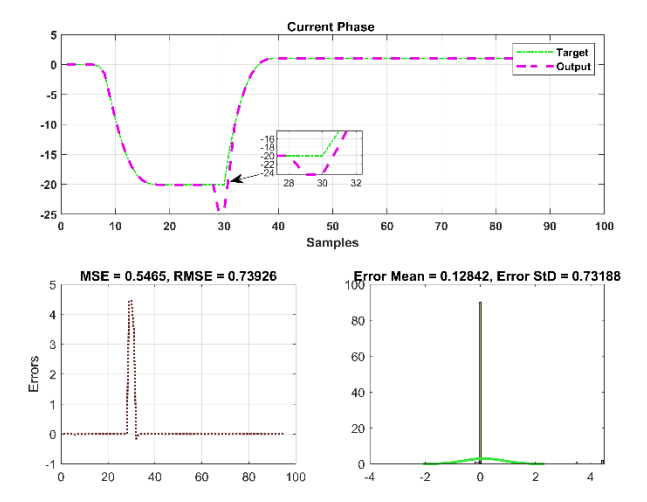


Figure 22 Neuro Fuzzy non-linear model control output for  $\theta_{Iy}$ .

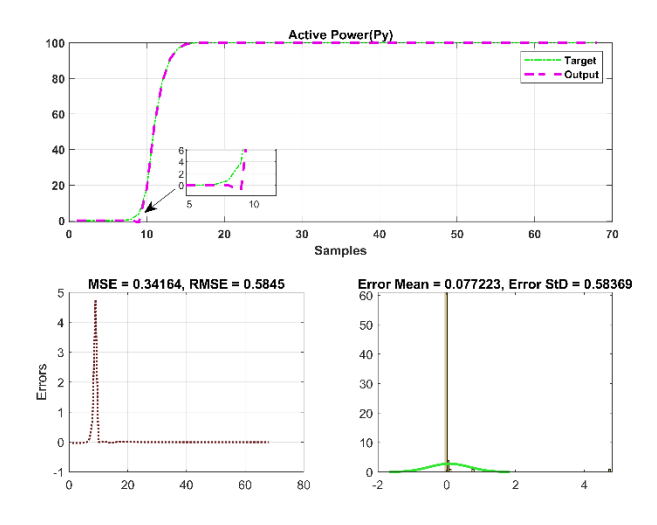


Figure 23 Neuro Fuzzy non-linear model control output for  $P_{v}$ .

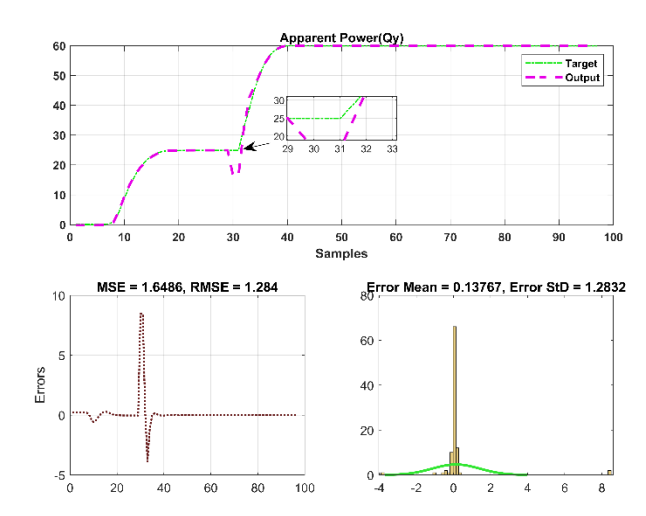


Figure 24 Neuro Fuzzy non-linear model control output for  $Q_y$ .

The difference in MSE between the linear and nonlinear systems is seen in Table 1. The nonlinear system, impacted by transients and residual nonlinearities, registers larger MSE whereas the linear system records lower MSE values. It is remarkable that both systems effectively converge towards the required reference outputs despite this mismatch. This demonstrates the efficiency of the control technique in controlling the complexity of the nonlinear system while guaranteeing the achievement of the specified performance goals.

Table 1 Linear and Non-linear error comparison

Outputs	Linear Model MSE	Non-Linear Model
		MSE
$f_{sys}$	0.30465	2.3826
$I_{\mathbf{y}}$	0.009567	1.4918
$\theta_{Iy}$	0.031592	0.5465
$P_{\nu}$	0.003991	0.3416
$\vec{Q_{v}}$	0.44256	1.6486

The reduction in mean square error (MSE) that we found for the linear model in our study as compared to the nonlinear model suggests that the neuro-fuzzy controller manages uncertainties and transients in the linear system well. The model's underlying linearity makes a control approach easier to implement, which enhances output tracking performance. But in the nonlinear model, the neuro-fuzzy controller finds it difficult to handle the complexity that nonlinearities bring, which results in a relatively higher MSE. In real-world situations when there are disruptions and outside influences, the neuro-fuzzy system's flexibility becomes essential. Although neuro-fuzzy controllers are excellent at managing uncertainties because they dynamically modify parameters in response to input data, the addition of nonlinearities, disturbances, and sensor noise can affect the mean square error (MSE) and even raise it because of the difficulties presented by nonlinear dynamics and outside factors. The resulting MSE depends on how well the system adjusts to this complexity and varies according to the details of the particular nonlinear plant as well as outside variables.

#### IV. NOVELTY

Our work presents a novel method for controlling synchronous generators through the use of an Artificial Neuro-Fuzzy Inference System with multiple inputs and multiple outputs. Compared with previous approaches based on traditional neural networks, our technology is more effective and provides better tracking and control. Since synchronous generators account for 95% of the world's energy production, this breakthrough is essential because it highlights the possibility of long-term, significant efficiency improvements and savings.

## V. CONCLUSION

In conclusion, this research explored the use of state feedback and neuro-fuzzy controllers in the control of both linear and nonlinear systems. The results show how this control schemes operate differently from one another.

The state feedback controller excels at offering accurate reference tracking with little error for linear systems. It is a reliable option for situations involving linear systems.

On the other hand, nonlinear systems pose unique problems such as transient responses and persistent nonlinearities. The neuro-fuzzy controller, however, exhibits a remarkable capacity to adjust to these difficulties. The nonlinear system eventually converges to the desired reference outputs despite the existence of a significantly higher mean square error (MSE), highlighting the adaptability and durability of this control strategy.

Future directions for research could include refining non-linear system control strategies, examining hybrid control techniques, applying the findings to real-world scenarios, expanding on system identification, creating reliable control protocols, and investigating the use of cutting-edge neural network architectures like Long Short-Term Memory (LSTM) and Recurrent Neural Networks (RNN). By utilizing deep learning and sequence modelling to improve control system performance, these subjects provide intriguing avenues for further research and practical

application, ultimately propelling the field of control theory forward.

#### NOMENCLATURE

Angle of the internal rotor

	6		
$f_{ heta}$	Rate at which the HV bus's voltage phase		
	changes		
$\omega_B$	The base speed of the rotor in rad/s		
Ω	The rotor speed per unit		
$D_r$	The rotor's damping constant		
M	The inertia moment		
$T_m$	Constant for Mechanical torque		
$T_{do}$ , $T_{qo}$	Direct-axis and quadrature-axis of coil		
$X_d, X_q$	d and q-axis synchronous reactance		
$X'_{d}, X'_{q}$	d and q-axis transient reactance		
$e_{fd}$	Excitation voltage of the generator field		
$e_d, e_q$	Emf in the coil's d and q axes		
$T_A$	Automatic regulator's time constant		
$K_{A}$	Automatic gain of a voltage regulator		
$\nu_t$	Magnitude of the stator voltage		
$T_e$	Constant for electric torque		
$\bar{\bar{n}}$	Nominal value		
$r_s, r_T$	Transformer armature and winding resistance		
$X_T$	Transformer leakage reactance		
$\nu_d$ , $\nu_q$	d and q-axis voltage		
ν	HV bus voltage magnitude		
$\iota_y$ , $\theta_{\iota y}$	The magnitude and phase of current		
$P_y$ , $Q_y$	Power, Both Active and Reactive		
$f_{sys}$	Frequency of system		
$v_{ref}$	Reference constant of an automatic voltage		
,	regulator		
Δ	Model uncertainties		
$I_2$	Identity matrix of 2 x 2		

#### REFERENCES

- [1] Ritonja J. Robust and adaptive control for synchronous generator's operation improvement. Automation and Control. 2020;.
- [2] Kasilingam G, Pasupuleti J. Bbo algorithm-based tuning of pid controller for speed control of synchronous machine. Turkish Journal of Electrical Engineering and Computer Sciences. 2016;24(4):3274–3285.
- [3] Kobayashi T, Yokoyama A. An adaptive neuro-control system of synchronous generator for power system stabilization. IEEE transactions on energy conversion. 1996;11(3):621–630.
- [4] Syahputra R, Soesanti I. Control of synchronous generator in wind power systems using neuro-fuzzy approach. In: Proceeding of International Conference on Vocational Education and Electrical Engineering (ICVEE); 2015. p. 187–193.
- [5] Higuchi Y, Yamamura N, Ishida M, et al. An improvement of performance for small-scaled wind power generating system with permanent magnet type synchronous generator. In: 2000 26th Annual Conference of the IEEE Industrial Electronics Society. IECON 2000. 2000 IEEE International Conference on Industrial Electronics, Control and Instrumentation. 21st Century Technologies; Vol. 2; IEEE; 2000. p. 1037–1043.
- [6] Hiskens IA, Pai M. Hybrid systems view of power system modelling. In: 2000 IEEE International Symposium on Circuits and Systems (ISCAS); Vol. 2; IEEE; 2000. p. 228–231.

- [8] Qing X, Karimi HR, Niu Y, et al. Decentralized unscented kalman filter based on a consensus algorithm for multi-area dynamic state estimation in power systems. International Journal of Electrical Power & Energy Systems. 2015;65:26–33.
- [9] Pal B, Chaudhuri B. Robust control in power systems. Springer Science & Business Media; 2006.
- [10] Phadke AG, Kasztenny B. Synchronized phasor and frequency measurement under transient conditions. IEEE transactions on power delivery. 2008;24(1):89–95.
- [11] Singh AK, Pal BC. Decentralized control of oscillatory dynamics in power systems using an extended lqr. IEEE Transactions on Power Systems. 2015;31(3):1715–1728.
- [12] Ghahremani E, Kamwa I. Local and wide-area pmu-based decentralized dynamic state estimation in multi-machine power systems. IEEE Transactions on Power Systems. 2015; 31(1):547–562.
- [13] Yue D, Han QL, Peng C. State feedback controller design of networked control systems. In: Proceedings of the 2004 IEEE International Conference on Control Applications, 2004.; Vol. 1; IEEE; 2004. p. 242–247.
- [14] Bugajski DJ, Enns DF. Nonlinear control law with application to high angleof-attack flight. Journal of Guidance, Control, and Dynamics. 1992;15(3):761–767.
- [15] Natsiavas S. Analytical modeling of discrete mechanical systems involving contact, impact, and friction. Applied Mechanics Reviews. 2019;71(5):050802.
- [16] Dangelmayr G, Neveling M, Armbruster D. Structurally stable phase portraits for the five-dimensional lorenz equations. Zeitschrift f'ur Physik B Condensed Matter. 1986;64:491–501.
- [17] Sandhu GS, Rattan KS. Design of a neuro-fuzzy controller. In: 1997 IEEE international conference on systems, man, and cybernetics. Computational cybernetics and simulation; Vol. 4; IEEE; 1997. p. 3170–3175.

#### **AUTHORS**

ISSN: 1673-064X

Raheel Aslam – Master of Science from Department of Electrical Engineering, Pakistan Institute of Engineering and Applied Sciences, Islamabad, currently doing Ph.D. at School of Automation, South China University of Technology, Guangzhou, Guangdong, China, ORCID iD: 0009-0004-5585-4051.

Alisha Khalid – Studying Ph.D. at School of Optoelectronic Engineering, Changchun University of Science and Technology, Zhongshan, Guangdong, China. ORCID iD: 0000-0003-4273-7783.

**Abid Aman**– Studying Ph.D. at School of Automation, South China University of Technology, Guangzhou, Guangdong, China. ORCID iD: 0009-0002-3034-785X.

**Toqeer Ahmed** – Studying Ph.D. at School of Automation, South China University of Technology, Guangzhou, Guangdong, China.

**Kanwal Waqar** – Studying Ph.D. at School of Automation, South China University of Technology, Guangzhou, Guangdong, China. ORCID iD: 0000-0001-6599-3494

**Mohammad Rasel Amin**– Studying Ph.D. at School of Automation, South China University of Technology, Guangzhou, Guangdong, China. ORCID iD: 0009-0005-0152-0264

Correspondence Author – Raheel Aslam- Master of Science from Department of Electrical Engineering, Pakistan Institute of Engineering and Applied Sciences, Islamabad, currently doing Ph.D. at School of Automation, South China University of Technology, Guangzhou, Guangdong, China, ORCID iD: 0009-0004-5585-4051.